IMMUNOLOGY

Epitope-directed antibody selection by site-specific photocrosslinking

Longxin Chen[1,2]*, Chaoyang Zhu[1,3]*, Hui Guo[1], Runting Li[2], Limeng Zhang[2], Zhenzhen Xing[2], Yue Song[2], Zihan Zhang[1,2], Fuping Wang[1], Xiaofeng Liu[1,3], Yuhan Zhang[1], Runlin Z. Ma[2,3], Feng Wang[1†]

Currently, there are no methods available offering solutions to select and identify antibodies binding to a specific conformational epitope of an antigen. Here, we developed a method to allow epitope-directed antibody selection from a phage display library by photocrosslinking bound antibodies to a site that specifically incorporates a noncanonical amino acid, *p*-benzoyl-L-phenylalanine (pBpa), on the target antigen epitope. By one or two rounds of panning against antibody phage display libraries, those hits that covalently bind to the proximity site of pBpa on specific epitopes of target antigens after ultraviolet irradiation are enriched and selected. This method was applied to specific epitopes on human interleukin-1β and complement 5a. In both cases, more than one-third of hits identified bind to the target epitopes, demonstrating the feasibility and versatility of this method.

INTRODUCTION

Monoclonal antibodies have become a major source of therapeutics to treat a variety of clinical indications (*1*–*3*). Mouse immunization and phage display technologies using large antibody sequence diversity have been developed and routinely used to select antibodies with high affinity and specificity (*4*). Antibody generation by mouse hybridoma technology typically starts with immunizing mice with peptides or proteins a few times, followed by extracting spleen cells from responsive animals to generate hybridomas by cell fusion. The hybridoma cells secreting antibodies with desired functions will be selected. In contrast, phage display technology enriches and selects hits from large preconstructed antibody phage display libraries by rounds of panning against the target antigen in vitro. Both methods are usually effective in identification of antibody binders with high affinities. However, therapeutic antibodies often require binding to a specific epitope in an antigen to exert their functions, e.g., blocking a ligand-receptor interaction, eliciting agonistic activities on receptors, and recruiting two proteins to form a complex (*5*). This epitope dependence exerts a great challenge to the current selection methods. Typically, one has to screen hundreds of hits from phage panning or hybridoma clones generated from mouse immunization to hopefully identify the antibodies binding to the desired epitopes (*6*, *7*). Unfortunately, the epitopes on antigens are not equal in eliciting antibody responses. Antibodies produced from mouse immunization of a whole antigen are usually enriched to immune-dominant B cell epitopes, often diminishing the odds of identifying antibodies binding the desired epitopes with low response (*8*, *9*). In addition, antibodies from immunization of the linear peptide containing the epitope sequence may not bind to the conformational epitope. Phage library panning technology faces a similar epitope bias issue, because its selection relies on binding affinities. Antibody clones with high affinity dominate the selection pool after rounds of enrichment, which limits both the diversity of antibody sequences identified and the corresponding binding epitopes. Those hits with low to medium affinities are very likely masked by the strong binders and are therefore difficult to be selected and usually lost during hit picking. Retaining more sequence diversity in the early stage is particularly important for development of therapeutic antibodies because affinity is only one of many criteria (physiochemical properties, stability, pharmacokinetics, immunogenicity, etc.) for selection of drug candidates. One can intentionally decrease selection stringency to save those "weak hits." However, it would require further screening and optimizing a large number of hits, which is not efficient if most of those hits do not bind to the target epitopes. Despite great progress in antibody discovery technology development, there is still no simple solution to identify the hits binding to specifically targeted conformational epitopes.

The noncanonical amino acids (ncAAs) *p*-benzoyl-L-phenylalanine (pBpa) and *p*-azido-L-phenylalanine (pAzF) have been incorporated into proteins by genetic codon expansion method and have been shown to covalently cross-link proteins of proximity upon ultraviolet (UV) irradiation (*10*–*13*). Here, we took advantage of this reactivity and developed a method that allows us to easily select antibodies binding to specific conformational epitopes of antigens by cross-linking bound antibodies from a library to site-specific incorporated pBpa on the target antigen epitope.

RESULTS

Incorporation of an ncAA with photocrosslinking reactivity in the target epitope

Interleukin-1β (IL-1β) is an important cytokine that mediates inflammatory responses and a variety of physiological activities. Canakinumab is a monoclonal antibody blocking the interaction of human IL-1β with IL-1 receptor (IL-1R) and was approved by the U.S. Food and Drug Administration to use in clinic. On the basis of the crystal structure of the canakinumab–IL-1β complex [Protein Data Bank (PDB): 4G6J], the antigen epitope that canakinumab binds includes Ser^{21}, Glu^{25}, Lys^{27}, Glu^{64}, Lys^{65}, Asn^{66}, and Asn^{129} (*14*). Among these, residues Glu^{64}, Lys^{65}, and Asn^{66} are in a flexible loop and form extensive interactions with CDR3 of V_H and CDR1 and CDR3 of V_L (fig. S1A). Another neutralizing antibody, gevokizumab,

[1]Key Laboratory of Protein and Peptide Pharmaceuticals, Institute of Biophysics, Chinese Academy of Sciences, Beijing 100101, China. [2]Molecular Biology Laboratory, Zhengzhou Normal University, Zhengzhou 450044, China. [3]School of Life Sciences, The University of Chinese Academy of Sciences, Beijing 100049, China.
*These authors contributed equally to this work.
†Corresponding author. Email: wangfeng@ibp.ac.cn

not only binds to a distinct epitope (PDB: 4G6M) but also could block the interaction between IL-1β and IL-1R and IL-1R accessory protein (IL-1RAcP) (fig. S1B) (*14*, *15*). We selected IL-1β as the initial target and residues 63 to 66 as the target epitope to develop and validate the new selection method. Residues Ala^2 and Leu^7 of the antigen are greater than 13 Å away from loop 63–66 and do not form any direct interactions with canakinumab or gevokizumab and were therefore selected as negative controls of the undesired binding site (fig. S1).

A *Methanocaldococcus jannaschii* (Mj) tyrosyl–transfer RNA synthetase (MjTyrRS) mutant and $MjtRNA_{CUA}$ pair was previously evolved to efficiently suppress nonsense codon TAG in *Escherichia coli* by ncAA pBpa (*16*–*21*) and site-specifically incorporate pBpa into multiple proteins (*13*). pBpa can be activated to form covalently cross-linked product with proteins upon exposure to UV irradiation (Fig. 1A) (*22*, *23*). The plasmid encoding the IL-1β mutant gene with a permissive amber codon at 63, 64, 65, 66, 2, or 7 was generated (designated as 63pBpa, 64pBpa, 65pBpa, 66pBpa, 2pBpa, or 7pBpa, respectively). The plasmid was cotransformed into *E. coli* BL21 (DE3) along with the pBpaRS (containing mutations Y32G, V103L, E107P, D158T, and I159S in the context of MjTyrRS-$tRNA_{CUA}$ pair) encoded on a pEVOL vector (*24*). Only cells containing double plasmids expressed full-length protein in the presence of the pBpa, which were purified by nickel–nitrilotriacetic acid (Ni-NTA) chromatography, followed by size exclusion chromatography (SEC). Yields ranged from 8 to 43 mg/liter in 2× YT medium in the presence of 1 mM pBpa (fig. S2). Proteins were analyzed by SDS–polyacrylamide gel electrophoresis (PAGE) (Fig. 1B) and electrospray ionization mass spectrometry (ESI-MS; fig. S3, A to G) to confirm the incorporation of pBpa. IL-1β wild-type (WT) and mutant proteins migrated as a single band at ~19 kDa on an SDS-PAGE gel and exhibited the expected mass that is consistent with its amino acid sequence; no background incorporation in the absence of pBpa was observed (fig. S2A).

pBpa incorporated epitope can cross-link with antibodies bound in proximity after UV irradiation

We first examined the binding affinity of canakinumab to the IL-1β WT and the pBpa incorporated mutants. Among these mutants, 65pBpa lost its binding with canakinumab, suggesting that Lys^{65} of IL-1β forms critical interactions with the antibody or the side chain of 65pBpa generates unfavorable interactions with the antibody. The incorporation of pBpa at position 63, 64, 66, 2, or 7, however, did not affect the binding to canakinumab (figs. S4 and S5A). In comparison, gevokizumab, targeting a distinct epitope, bound to WT and all mutants indifferently (figs. S4 and S5B). Therefore, gevokizumab can be used as an off-target epitope control for the following study. Next, we evaluated the UV cross-linking activity of pBpa in the context of IL-1β mutants 63pBpa, 64pBpa, 66pBpa, 2pBpa, or 7pBpa. These mutants and WT IL-1β (0.5 mg/ml) were incubated with canakinumab (1 mg/ml) and exposed to UV (6 W, 365 nm) for up to 10 hours according to the method used in cross-linking studies of other proteins (*25*). The SDS-PAGE and Western blot results showed that mutants 63pBpa, 64pBpa, and 66pBpa formed covalently linked products with canakinumab light chain, while 2pBpa and 7pBpa (distal from the binding interface) did not (Fig. 1C and fig. S6A). MS data also support these results (fig. S7), which confirmed that pBpa in IL-1β can cross-link with a binding antibody in proximity under UV irradiation. As expected, there was no cross-linking with gevokizumab, which binds to a distinct site (more than 13 Å away from loop 63–66) under the same conditions (Fig. 1C and figs. S1 and S6B). This indicates that only when the distance is close enough (3 to 5 Å), the cross-linking between the antibody and pBpa in IL-1β can occur efficiently upon UV irradiation (fig. S8) (*26*). We selected 64pBpa, which showed the best cross-linking efficiency among mutants 63-66pBpa and 63pBpa (pBpa in its adjacent residue) for the following library selection experiments.

Epitope-directed selection against a human naïve antibody phage library

We previously built a multivalent single-chain Fv (scFv)–pIII phage display library using B cells from human peripheral blood mononuclear cells according to published methods (Supplementary Text) (*27*, *28*). This library has an antibody sequence diversity of ~10^9. An input of 10^{10} plaque-forming units (PFU) of phages was incubated for 4 hours with 63pBpa and 64pBpa that were precoated and blocked on plates, followed by 15-min UV irradiation (6 W, 365 nm). After three rounds of competitive washes [Dulbecco's phosphate-buffered saline (DPBS), 0.05% Tween 20, pH 7.4, plus WT IL-1β (0.1 mg/ml)], three rounds of low-pH washes (300 mM NaCl, 3% Tween 20, 100 mM glycine, pH 2.0) to remove noncovalently bound phages, and three rounds of PBS washes to neutralize pH, the covalently cross-linked phages were eluted by trypsin digestion (Fig. 2). The output phage pool was harvested and reinfected *E. coli* XL1-Blue for counting colony-forming units (CFU) and hit picking. As expected,

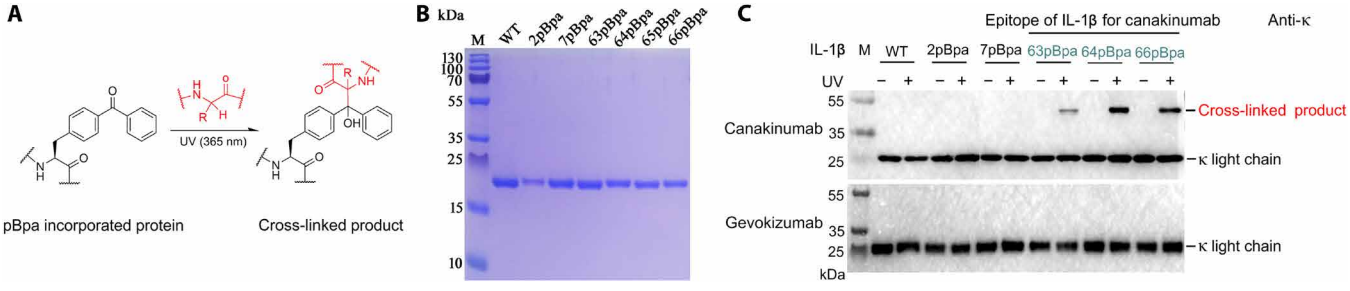

Fig. 1. Incorporation of pBpa in IL-1β and its reactivity with IL-1β binding antibodies. (**A**) Photocrosslinking chemistry scheme of pBpa. pBpa is activated to form cross-linked product upon exposure to UV irradiation. (**B**) SDS-PAGE of purified IL-1β WT and pBpa mutants. IL-1β WT and pBpa mutants can be readily overexpressed and purified by Ni-NTA plus SEC. (**C**) IL-1β–pBpa mutants cross-linked with canakinumab after treatment or nontreatment by UV irradiation. Mutants 63pBpa, 64pBpa, and 66pBpa formed covalently linked products with canakinumab light chain, while 2pBpa and 7pBpa (distal from the binding interface) did not. Western blot of IL-1β-pBpa mutants incubated with canakinumab or gevokizumab in the presence and absence of UV irradiation using anti-human κ light chain horseradish peroxidase (HRP; Invitrogen, 42-60-050214) (detecting canakinumab or gevokizumab) and exposed with enhanced chemiluminescence (ECL; Thermo Fisher Scientific, 35055).

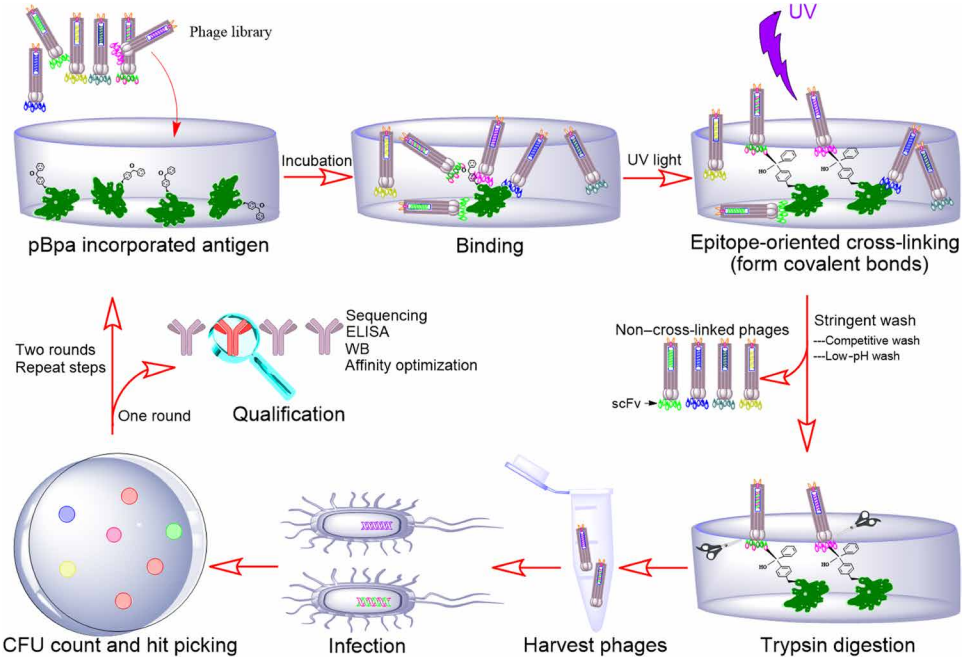

Fig. 2. Strategy of epitope-directed panning against phage display library. An input of 10^{10} PFU of phages was incubated for 4 hours with an antigen that was precoated and blocked on plates, followed by 15-min UV irradiation (6 W, 365 nm) (in the absence of UV as a negative control, designated as non-UV). After three rounds of competitive washes [PBS, 0.05% Tween 20, pH 7.4, plus WT protein (0.1 mg/ml)], three rounds of low-pH washes (300 mM NaCl, 3% Tween 20, 100 mM glycine, pH 2.0) to remove noncovalently bound phages, and three rounds of PBS washes to neutralize pH, the covalently cross-linked phages were eluted by trypsin digestion. The output phage pool was harvested and reinfected *E. coli* XL1-Blue for counting CFU and hit picking. The selected hits were sequenced and used to produce monoclonal phages for downstream analysis. This panning process can be repeated if further enrichment is necessary.

the output CFUs from panning of both mutants are low. Nevertheless, compared to the group without UV irradiation (designated as non-UV), the output CFU is three to four times higher, suggesting that a substantial portion of the output phage pool was covalently cross-linked with 63pBpa or 64pBpa (Table 1 and table S1). In contrast, panning against WT IL-1β using the same phage library and the same method exhibited a UV/non-UV output ratio of 1.2, indicating that no significant cross-linking happened without incorporated pBpa. In addition, monoclonal phages displaying the scFv of canakinumab and gevokizumab were generated and selected following the same protocol, respectively. The canakinumab-scFv phages exhibited a UV/non-UV output ratio of 3.8. In contrast, the gevokizumab-scFv phages exhibited a ratio of 1.1, indicating no significant number of phages cross-linked with IL-1β because it binds an epitope distant from where pBpa was incorporated.

Hit picking and analysis

We randomly picked 55 colonies from the hit pool of 63pBpa or 64pBpa and analyzed their sequences. The sequences are diverse with low homology (fig. S9). We selected 15 (7 and 8 from the hit pool of 63pBpa and 64pBpa, respectively) distinct sequences to generate monoclonal phages. The binding affinities of these phages to WT IL-1β and mutant 63pBpa or 64pBpa were analyzed by enzyme-linked immunosorbent assay (ELISA). As shown in Fig. 3 (A and B), more than half of phages from selection on 63pBpa or 64pBpa were cross-reactive with WT, although some of them showed reduced affinities. Two monoclonal phages with significant affinities to both WT IL-1β and 63pBpa or 64pBpa, respectively, were picked (designated as 63UV7 and 64UV63) and then incubated with 63pBpa or 64pBpa and processed with the panning procedure. After elution, the output CFUs of UV- and non–UV-treated groups were counted and compared. The CFU of UV-treated group is four to six fold higher than the non–UV-treated group (table S2), demonstrating that these monoclonal phages bind to the desired epitope and could cross-link with 64pBpa or 63pBpa upon UV irradiation. As a control, these phages did not show much difference on the CFUs between UV- and non–UV-treated groups against WT IL-1β (table S2). In addition, we generated $Lys^{63}Ala$, $Glu^{64}Ala$, $Lys^{65}Ala$, and $Asn^{66}Ala$ single mutants and a $Lys^{63}Ala$-$Asn^{66}Ala$ quadruple mutant of IL-1β (fig. S10). Phages 64UV63 and 63UV7 showed significantly lower affinities to some of these alanine mutants compared to the WT, 63pBpa, or 64pBpa, demonstrating that they bind to the targeted epitope (Fig. 3C and fig. S11). Next, we generated scFv-Fc fusion proteins and measured the binding affinities of these antibodies to the corresponding antigens by Biacore, which is consistent with the results from phage ELISA (fig. S12).

Epitope-directed selection against an antibody phage library from mouse immunization

Because mouse immunization is a popular approach to generate antibodies with high affinity and selectivity against an antigen, we applied the epitope-directed antibody selection method to the phage library produced from mouse immunization approaches. Mice were immunized with WT IL-1β for three times using a routine protocol (*28*). Once the antibody titer in serum was confirmed, their spleens were collected and used to generate phage display libraries (*27*, *28*). These libraries were then used for epitope-directed panning using a similar method described in the above sections, except that two

Table 1. UV/non-UV output ratio of hit pools from panning a human naïve antibody phage library against 63pBpa and 64pBpa. The *P* value of pBpa mutant group versus negative antigen control and positive phage control group versus negative phage control group. **P* < 0.05. The statistical analysis was based on the UV/non-UV output ratios listed here and in table S1, which are from two independent repeats.

Sample	UV output (CFU)	Non-UV output (CFU)	UV/non-UV output ratio
Hit pool from panning against 64pBpa	268	86	3.1*
Hit pool from panning against 63pBpa	981	261	3.7*
Canakinumab-scFv phage against 63pBpa (positive phage control)	6400	1696	3.8*
Gevokizumab-scFv phage against 63pBpa (negative phage control)	8650	7900	1.1
Hit pool from panning against WT IL-1β (negative antigen control)	776	648	1.2

rounds of panning were applied against 64pBpa to further enrich the hits. The output CFUs from the UV-treated group are about five to nine times higher than those of the non–UV-treated group (Table 2 and table S3). In contrast, the UV/non-UV ratios of the hit pool and the selected hits are all around 1 when WT IL-1β was used as the antigen (table S4).

We randomly picked 47 colonies from the hit pool and analyzed their sequences. Seven sequence families were identified on the basis of homology (fig. S13). We selected one representative clone from each family and produced monoclonal phages (except for one clone that yielded very low phage titer after production). We then examined the output CFUs of these selected phages after one round of panning with or without UV irradiation. As shown in Table 2 and table S3, two of the six selected monoclonal phages exhibited a UV/non-UV ratio larger than 3 against 64pBpa, demonstrating their ability to cross-link with the target epitope. As a control, these phages did not show significant difference on the CFUs between UV and non-UV groups against WT IL-1β (table S4).

Epitope-directed selection of hC5a-specific antibodies showing the versatility of the method

Together, we have established a method to allow facilely selecting antibody clones with high sequence diversity binding to a specific

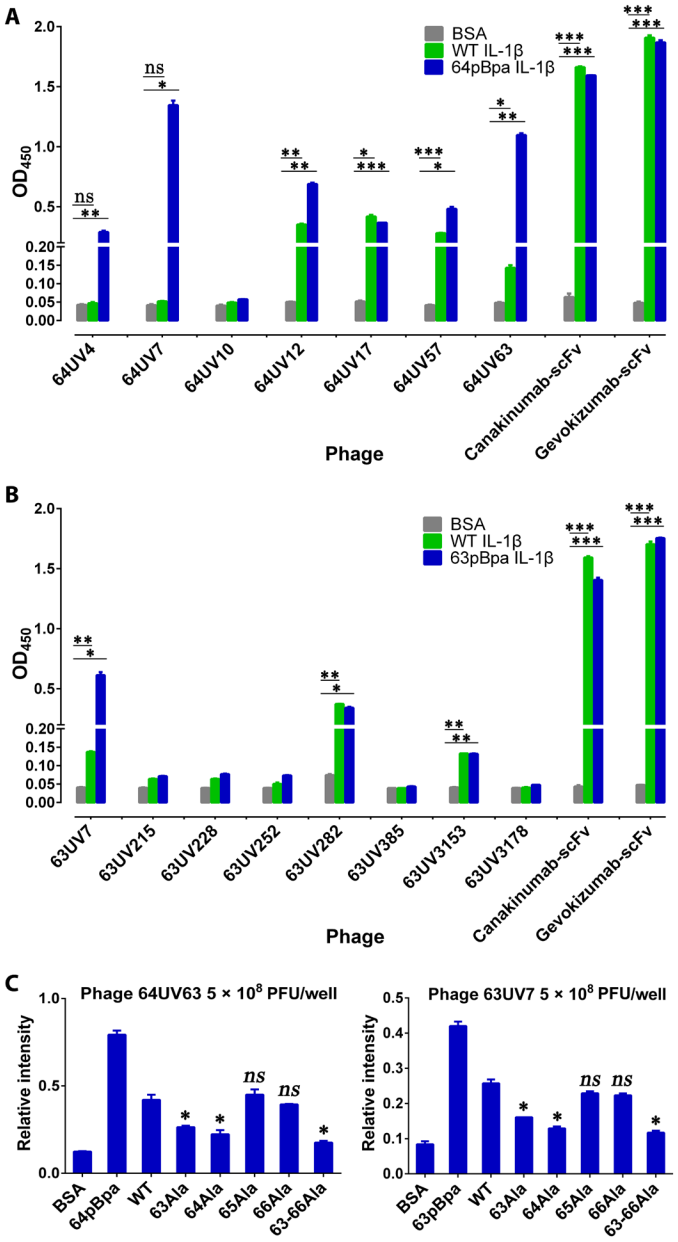

Fig. 3. Binding of monoclonal phage hits on WT and mutant IL-1β. ELISA of phage hits from panning pool of 64pBpa (**A**) and 63pBpa (**B**). The *P* value of WT or pBpa mutant groups versus bovine serum albumin (BSA) group. Among the 15 selected monoclonal phages from the phage pool by panning against 63pBpa and 64pBpa, more than half were cross-reactive with WT. (**C**) ELISA of phage hits 64UV63 and 63UV7 from panning against 64pBpa and 63pBpa, respectively. The bound phages were detected and quantified by adding anti-M13 HRP (GE Healthcare, 27-9421-01) and exposed with trimethylboron (TMB; Invitrogen, 002023). The *P* value of alanine mutant groups versus WT group. Phages 64UV63 and 63UV7 showed significantly lower affinities to the alanine mutants compared to the WT, 63pBpa, or 64pBpa, demonstrating that they bind to the target epitope. **P* < 0.05, ***P* < 0.01, ****P* < 0.001, $^{ns}P \geq 0.05$.

epitope in IL-1β from phage display libraries. As therapeutic antibodies often require binding to a specific epitope in an antigen to exert their functions, this method could potentially facilitate antibody drug development. To demonstrate the versatility of this method on other therapeutic targets, we applied it to another antigen, human

Table 2. UV/non-UV output ratio of the hit pool and monoclonal phages from panning an antibody phage library (generated by mouse immunization) against 64pBpa. The *P* value of pBpa mutant group versus negative antigen control group (in table S4). $^{*}P < 0.05$, $^{ns}P \geq 0.05$. The statistical analysis was based on the UV/non-UV output ratios listed here and in tables S3 and S4, which are from two independent repeats.

Sample	UV output (CFU)	Non-UV output (CFU)	UV/non-UV output ratio
Hit pool from panning against 64pBpa	3500	380	9.2*
i64UV9 phage	7500	1400	5.4*
i64UV120 phage	6600	1900	3.5*
i64UV5 phage	296	312	0.9^{ns}
i64UV40 phage	7900	7400	1.1^{ns}
i64UV104 phage	1300	980	1.3^{ns}
i64UV110 phage	1240	1020	1.2^{ns}

complement 5a (hC5a) (*29*–*31*). hC5a is a potential target for therapeutics to treat multiple diseases and syndromes such as anti-neutrophil cytoplasmic antibody–associated vasculitis, atypical hemolytic uremic syndrome, systemic lupus erythematosus, rheumatoid arthritis, and ischemia/reperfusion injury (*32*). To develop a therapeutic antibody targeting hC5a, it is desirable to not only efficiently block the binding of hC5a to C5a receptor (C5aR) but also be highly selective to hC5a versus hC5. By analyzing the crystal structures of human C5a (PDB: 3HQA) and C5 (PDB: 3CU7), we identified an epitope (Ser^{16}, Val^{17}, Val^{18}, Lys^{19}, and Lys^{20}), which is involved for the interaction with C5aR (*33*, *34*), but is buried inside the surface of hC5 (fig. S14). Therefore, antibodies binding to this epitope of hC5a are less likely to bind to hC5. Moreover, the sequence of this epitope is highly conserved between human, monkey, and rodent, which suggests that antibodies binding to this epitope are very likely cross-reactive among species (fig. S15).

We generated and characterized a Val^{18}pBpa mutant of hC5a (designated as 18pBpa) (figs. S3, H and I, and S16) and used it for epitope-directed antibody selection. We performed panning against phage display libraries generated from spleens of mice immunized with hC5a. Following the selection procedure described above, after two rounds of panning against 18pBpa, the UV/non-UV output ratio was larger than 13, suggesting that a significant portion of the output phage pool was covalently cross-linked with the antigen (table S5). We selected 25 colonies from the hit pool and analyzed the sequences. Sequences with correct scFv sequence assemblies were clustered on the basis of homology (fig. S17). Hit hC5a-35 was selected from the cluster with the most abundant homologous sequences. Although it only showed modest affinities to hC5a and low affinity to 18pBpa, its UV/non-UV output CFU ratio is larger than 3 (Fig. 4A). After affinity maturation on WT hC5a using a secondary phage library generated by random mutagenesis (Supplementary Text), a strong binder hC5a-35-E02 phage (E02) was identified with high affinity to hC5a and significantly increased UV/non-UV output ratio of 8.6 (Fig. 4, B and C). We generated Val^{18}Ala and Lys^{19}Ala single mutants and a Val^{18}Ala-Lys^{19}Ala double mutant of hC5a (fig. S18). E02 showed significantly lower affinities to these alanine mutants compared to the WT hC5a, demonstrating that it binds to the target epitope (Fig. 4B). As expected, E02 showed much lower affinity to hC5 (fig. S19A) but similar binding affinity to mouse complement 5a (mC5a) (fig. S20A). Next, we generated an E02-scFv-Fc fusion protein (fig. S21) and measured its binding affinities to hC5a, Val^{18}Ala, Lys^{19}Ala, Val^{18}Ala-Lys^{19}Ala, hC5, and mC5a. The binding affinity profile corresponds to the results of E02 phages (Fig. 4D and figs. S19B, S20B, and S22). Western blot results also demonstrated that 18pBpa formed a covalently linked product with E02-scFv-Fc fusion protein, while WT hC5a did not (Fig. 4E).

DISCUSSION

We developed an approach for facile selection and identification of antibodies binding to a specific epitope of an antigen. The foundation of this method is site-specific incorporation of an ncAA with photocrosslinking reactivity in or near the epitope of interest by genetic code expansion. The mutant antigen is then used for panning against antibody phagemid display libraries produced from B cell repertoires of different sources. The conventional phage selection method relies on the affinities of antibody-displayed phages to the whole antigen. After rounds of panning, those clones with high affinities are enriched and identified by sequencing. In contrast, in our approach, the antigen incorporated with a photocrosslinker could form a covalent bond with antibody-displayed phages that bind to the target epitope after UV irradiation. Those phages binding to the nontargeted epitopes could not cross-link with the antigen and are eliminated during stringent washing steps. Thus, only the phages binding to the target epitope are enriched and selected, independent on their initial binding affinities. We are aware that in some scenarios, nonspecific binders may not be completely washed off and become background noise. Nevertheless, by optimizing washing stringency, the ratio of UV/non-UV CFU is significant enough and affords a high probability of identifying the hits binding to the target epitope. By this approach, in the case of IL-1β, one-third of the hits identified after two rounds of panning bound to the target epitope. All identified hits were cross-reactive with WT IL-1β. In comparison, none of the hits bound to the epitope using conventional panning methods (Supplementary Text) (*35*). Furthermore, the hits identified retain higher sequence diversity than those from conventional phage selection (fig. S23). This high sequence diversity is advantageous for downstream hit optimization and candidate selection.

To demonstrate the versatility of this approach, we performed epitope-directed antibody selection against another therapeutic target, hC5a. Once again, using a rationally designed Val^{18}pBpa mutant, we identified hits binding to the target epitope. Another advantage of this method is that once the primary hit pool is obtained, it is compatible with current approaches for downstream affinity optimization (*35*, *36*). After affinity optimization using a secondary phage library generated by random mutagenesis, we obtained a candidate antibody exhibiting high affinity and selectivity to the epitope, which helped to differentiate its binding to hC5a from hC5 and gain species cross-reactivity by design.

Last, this method could be more advantageous when the target epitope resides in a transmembrane protein, such as an ion channel or G protein–coupled receptor (GPCR), which is a very important but challenging therapeutic target class (*37*, *38*). In these cases, the antigen with active conformation is difficult to isolate from the cell

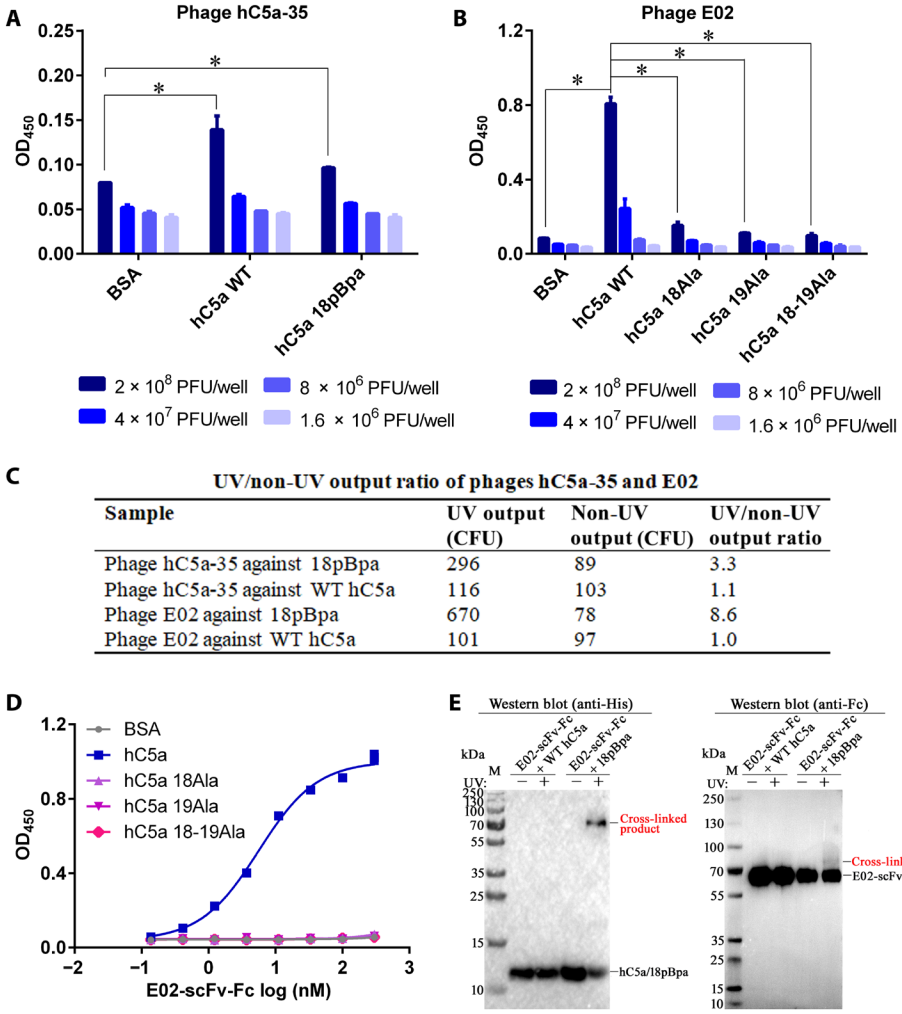

Fig. 4. Selection of hC5a-specific neutralizing antibodies. (**A**) ELISA of phage hC5a-35 on WT hC5a and 18pBpa. The *P* value of group WT or 18pBpa group versus BSA group, **P* < 0.05. (**B**) ELISA of phage E02 on alanine mutants compared to WT hC5a. The *P* value of WT group versus alanine mutant groups or BSA group, **P* < 0.05. E02 showed significantly lower affinities to the alanine mutants compared to the WT hC5a, demonstrating that it binds to the target epitope. (**C**) UV/non-UV output ratio of phages hC5a-35 and E02 against 18pBpa. hC5a-35-E02 phage was identified with high affinity to hC5a and significantly increased UV/non-UV output ratio of 8.6. (**D**) E02-scFv-Fc binding profile on hC5 and alanine mutants. Consistent with the phage binding profile, E02-scFv-Fc showed significantly lower affinities to the alanine mutants compared to the WT hC5a, demonstrating that it binds to the target epitope. (**E**) Western blot results showed E02-scFv-Fc covalently bound to 18pBpa. Western blot detecting antigen, antibody, and cross-linked product for WT versus 18pBpa in the presence or absence of UV using anti-His to detect hC5a (left) and anti-human Fc HRP (SeraCare, 5220-0279) to detect antibody (right). Cross-linked products were labeled.

membrane. Therefore, phage panning against the antigen on the cell surface is usually required, which is technically difficult. The rate of success is extremely low to identify hits binding to cell surface antigens due to high background of nonspecific binders, not to mention identifying the hits binding to the target epitopes. In future, we plan to apply our epitope-directed panning method on transmembrane protein targets to take advantage of enhanced signal-to-noise ratio through UV-activated cross-linking.

MATERIALS AND METHODS

All procedures using mice were reviewed and approved by the Laboratory Animal Center of Institute of Biophysics, Chinese Academy of Sciences (CAS), and were performed using protocols in accordance with the relevant guidelines and regulations.

All statistical analyses were performed using GraphPad Prism, and data were averaged across subjects and tested for significance by paired-sample *t* test. Bar height denotes the mean average of sample-specific relative affinity values, and values are plotted as means ± SEM from two repeats.

Construction of plasmids of WT hIL-1β, hC5a, and their mutants

The Gibson assembly method was applied to quickly generate all plasmids of this work (*39*). The open reading frames of human *IL-1*β and *C5a* genes fused with a 6× histidine at the C terminus were amplified from pUC57–IL-1β and pUC57-hC5a (generated by DNA synthesis) with primers IL-1β–WT–F/R and hC5a-WT-F/R (Supplementary Text), respectively, and inserted into the linearized pET28a vector (Novagen, 69864-3) (digested with *Nco* I and *Nhe* I)

by Gibson assembly. Site-directed mutagenesis was performed to generate plasmids pET28a–IL-1β–2TAG, pET28a–IL-1β–7TAG, pET28a–IL-1β–63TAG, pET28a–IL-1β–64TAG, pET28a–IL-1β–65TAG, pET28a–IL-1β–66TAG, and pET28a-hC5a-18TAG using the Hieff Clone Plus One Step Cloning Kit (Yeasen Biotech, 10911) according to the manufacturer's protocol. These plasmids were used to express IL-1β and hC5a mutants incorporated with pBpa (J&K Scientific, 204322, CAS104504-45-2) (Supplementary Text). The same method was applied to the construction of pET28a–IL-1β–2Ala, pET28a–IL-1β–7Ala, pET28a–IL-1β–63Ala, pET28a–IL-1β–64Ala, pET28a–IL-1β–65Ala, pET28a–IL-1β–66Ala, pET28a–IL-1β–63-66Ala, pET28a-hC5a-18Ala, pET28a-hC5a-19Ala, and pET28a-hC5a-18-19Ala, which was used to express alanine mutants of IL-1β and hC5a (Supplementary Text).

Expression and purification of hIL-1β, hC5a, and their mutants

To overexpress IL-1β or hC5a WT and alanine mutants, an overnight culture of BL21 (DE3) *E. coli* was transformed with the corresponding plasmid in the pET28a vector and was diluted 100-fold into 1 liter of 2× YT medium supplemented with kanamycin (50 μg/ml) at 37°C. The cells were cultured for 3 to 5 hours when the OD_{600} (optical density at 600 nm) reached 0.6, and 0.5 mM isopropyl-β-D-thiogalactopyranoside (IPTG) was added to induce expression at 30°C at 220 rpm overnight. To overexpress pBpa incorporated mutants of hIL-1β and hC5a, an overnight culture of BL21 (DE3) *E. coli* cotransformed with pEVOL-pBpaRS and the corresponding plasmid containing the amber codon were cultured in 1 liter of 2× YT medium supplemented with kanamycin (50 μg/ml) and chloromycetin (25 μg/ml). The cells were allowed to grow for 3 to 5 hours when the OD_{600} reached 0.6, and 0.5 mM IPTG, 1 mM pBpa, and 0.2% L-arabinose (m/v) in final concentration were added to express pBpa incorporated proteins. The cells were grown for an additional 30 hours at 30°C at 220 rpm overnight before harvesting by centrifugation at 6000*g* for 10 min. The cell pellet was lysed by sonication, and the resulting cell lysate was clarified by centrifugation at 13,000*g* for 30 min at 4°C. IL-1β or hC5a WT and mutants were purified on Ni-NTA resin (GenScript, L00250) following the manufacturer's instructions. Then, the proteins were further purified through SEC in DPBS buffer. Briefly, the protein sample after Ni-NTA chromatography purification was loaded on a Superdex 75 10/300 GL column (GE Healthcare) and eluted with DPBS. The absorbance at 280 nm was recorded and plotted as a function of elution time. The major peak was collected for downstream characterization and studies.

Construction of expression plasmids of full-length IgG and scFv-fc fusions

The heavy and light chains of the corresponding antibody sequence were generated by DNA synthesis and overlap polymerase chain reaction amplification, which were then ligated into the linearized pFUSE expression vector (InvivoGen) by Gibson assembly method to afford pFUSE-HC and pFUSE-LC. The corresponding pFUSE-HC and pFUSE-LC plasmid pair was cotransformed into human embryonic kidney (HEK) 293F cells for expression. The scFv was generated by DNA synthesis using V_H and V_L of the corresponding antibody sequence and fused with human immunoglobulin G1 (IgG1) Fc by a glycine-serine linker and ligated into the linearized pFUSE expression vector. The sequences of all plasmids were confirmed by DNA sequencing (GENEWIZ) (Supplementary Text).

Expression and purification of IgG antibodies and scFv-Fc fusion proteins

The genes containing the heavy and light chains of the IgGs or scFv-Fc fusions were expressed by transient transfection in HEK 293F cells (Thermo Fisher Scientific, R79007). The HEK 293F cells were cultured in shaker flasks containing FreeStyle medium (Thermo Fisher Scientific, 12338026) and shaken at 125 rpm at 37°C, with 5% CO_2. HEK 293F cells were grown up to a density of 2×10^6 cells/ml and were transfected with the light chain/heavy chain plasmids or scFv-Fc fusion plasmids and 293Fectin at a ratio of 1:2:6 or 1:2 following the manufacturer's instructions. The expression media were harvested and sterile-filtered twice every 48 hours after transfection to collect the secreted proteins. The antibodies or scFv-Fc fusion proteins were purified by protein A chromatography (GenScript, L00210) (*40*). Briefly, collected supernatant was loaded onto a protein A column twice, which was pre-equilibrated in DPBS. After washing with 10 column volumes of DPBS, the protein sample bound to the column was eluted with elution buffer (0.1 M glycine, 0.1 M NaCl, pH 2.7). Immediately after elution, tris-HCl (100 mM final concentration) was added to adjust the pH to 7.4. The eluted protein was then concentrated using Amicon centrifugal filters (Millipore) and exchanged into DPBS (pH 7.4). Then, the proteins were further purified through SEC.

Molecular weight determination by ESI Q-TOF

MS analysis of proteins was performed on an Agilent 6530 ESI quadrupole time-of-flight (Q-TOF) mass spectrometer (*41*). Briefly, liquid chromatography (LC)–MS analysis was performed using an Agilent Q-TOF mass spectrometer in line with an Agilent 1290 HPLC system. Five microliters of protein (about 1 μg/μl) was loaded onto a reversed-phase column (300SB-C8, 2.1 mm × 50 mm, 3.5-μm particle) (Agilent Technologies, Santa Clara, CA). The sample was then eluted over a gradient (2% B for 2 min to waste, 2 to 50% B for 6 min, 50 to 90% B for 4 min, 90% B for 4 min, and then decreased to 2% B for 1.1 min, where B is 100% acetonitrile, 0.1% formic acid and A is water with 0.1% formic acid) at a flow rate of 0.2 ml/min and introduced online into the Q-TOF mass spectrometer using electrospray ionization. MS data were analyzed by MassHunter qualitative software with Biocom firm workflow.

Enzyme-linked immunosorbent assay

Protein sample (0.1 μg) in 100 μl of DPBS was coated on a 96-well plate (Corning Costar, 2592) at 4°C overnight. The plate was blocked with 200 μl of 3% non-fat milk solution in DPBST (DPBS, 0.25% Tween 20) for 2 hours at 37°C. Samples (first antibodies or phages) were incubated with 3% non-fat milk in DPBST for 2 hours at 37°C. Wells were washed four times with 200 μl of DPBST. Subsequently, horseradish peroxidase (HRP)–conjugated secondary antibody was added at a dilution in blocking solution and incubated for 1 hour at 37°C. Wells were then washed five times with 200 μl of DPBST. A 100-μl working solution of QuantaBlu (Thermo Fisher Scientific, 15169) or trimethylboron (TMB; Invitrogen, 002023) was added to each well and incubated for 10 to 30 min at room temperature before plates were read (*42*).

Western blot analysis

Samples were subjected to SDS-PAGE on polyacrylamide gels. After electrophoresis, proteins were stained with Coomassie brilliant blue and transferred onto polyvinylidene difluoride filter membrane

(Bio-Rad, 1620177) for Western blot analysis. The membranes were blocked with 10 ml of blocking solution (5% non-fat milk in DPBST) for 2 hours and then incubated at room temperature for 2 hours with first antibody in blocking solution. Membranes were washed three times in DPBST, then incubated at room temperature for 1 hour with 1:5000 dilute secondary antibody conjugated with HRP in DPBST in blocking solution, and finally washed with DPBST. Signals were generated by using enhanced chemiluminescence (ECL) reagent (Thermo Fisher Scientific, 35055) and detected with a Tanon 5200 system.

Construction of phage display library

Phage display libraries were constructed using the published methods (*27*, *28*). Briefly, to construct a human naïve phage library, white blood cells from healthy donors were isolated by sucrose density centrifuge, and their total RNA was extracted (QIAGEN, 74104) and reverse-transcribed into complementary DNA (cDNA) library. To construct a mouse immunization library, Balb/c mice were immunized by WT IL-1β or hC5a for three times with 2-week intervals. Total RNA from mouse spleen was extracted 2 weeks after the third immunization and used as the template for reverse transcription to construct cDNA library. The cDNA libraries were then used as templates to generate scFv phage display library using the phagemid vector pSEXRTL2. The libraries were packaged into scFv-pIII phages using hyperphage M13KO7Δ pIII (PROGEN, catalog no, PRHYPE).

Phage production

E. coli (XL1-Blue) carrying the phagemids were inoculated in 20 ml of 2× YT medium with ampicillin (100 μg/ml) and tetracycline (15 μg/ml; no glucose) and cultured at 37°C, 220 rpm until OD_{600} reached 0.5. Twenty multiplicity of infection (MOI) hyperphages were added to infect cells at 37°C, 120 rpm for 1 hour. The infected cells were spun down and cultured in 40 ml of 2× YT medium with ampicillin (100 μg/ml), tetracycline (15 μg/ml), and kanamycin (50 μg/ml) at 30°C, 260 rpm for 13 hours.

The culture was centrifuged at 4000*g* for 10 min to pellet down cells. Clear supernatant was transferred to a new tube and centrifuged at 10,000*g* for 20 min. The 5× phage precipitating buffer [polyethylene glycol, molecular weight 800 (PEG 8000)/NaCl: 100 g of PEG 8000, 73.3 g of NaCl, ddH_2O added to 500 ml] was added and incubated on ice for 4 hours. Phages were harvested by centrifugation at 10,000*g* at 4°C for 20 min and resolubilized by adding 1 ml of DPBS and incubated for 15 min at room temperature. The centrifugation and solubilization steps were repeated one more time to collect phage solution in 500 μl of DPBS.

Epitope-directed phage panning

The pBpa incorporated mutant or WT proteins were diluted to 0.1 μg per well in 100 μl of DPBS in a 96-well plate and incubated at 4°C overnight. Wells were blocked with 200 μl of blocking solution (3% non-fat milk in DPBST) at 37°C for 2 hours after washing with DPBST twice. After aspirating the wells, phages in 100 μl of blocking solution were added in each well and incubated at 37°C for 2 hours. The wells were aspirated and 100 μl of DPBS was added in each well. The wells with non-UV treatment were plated on ice at 4°C for 15 min, and the wells with UV treatment were plated on ice at 4°C and irradiated with UV light from a 6-W, 365-nm light (CBIO Science and Technology, CBIO-UV2A) for 15 min. The wells were aspirated and then washed sequentially with 200 μl of DPBST, 200 μl of competitive buffer (WT protein, 100 μg/ml in DPBST), 200 μl of acidic buffer (300 mM NaCl, 3% Tween 20, 100 mM glycine, pH 2.0), and DPBST for three times. After washing steps, 105 μl of trypsin (1.75 μg/ml) was added in each well to digest for 15 min at room temperature to release phages from the cross-linked phage-antigen complex. The collected phages from each well were incubated with 3 ml of *E. coli* XL1-Blue at $OD_{600} \approx 0.5$ for 1 hour to infect cells. Ten microliters of bacteria culture was then used in titer count on a 100-mm 2× YT solid medium plate with ampicillin/tetracycline/10% glucose (m/v) and incubated at 37°C overnight, and the rest of the culture was plated on a large square ampicillin/tetracycline/glucose plate and incubated at 37°C overnight.

SUPPLEMENTARY MATERIALS

Supplementary material for this article is available at http://advances.sciencemag.org/cgi/content/full/6/14/eaaz7825/DC1

View/request a protocol for this paper from *Bio-protocol*.

REFERENCES AND NOTES

1. Z. Elgundi, M. Reslan, E. Cruz, V. Sifniotis, V. Kayser, The state-of-play and future of antibody therapeutics. *Adv. Drug Deliv. Rev.* **122**, 2–19 (2017).
2. P. Sharma, J. P. Allison, The future of immune checkpoint therapy. *Science* **348**, 56–61 (2015).
3. M. X. Sliwkowski, I. Mellman, Antibody therapeutics in cancer. *Science* **341**, 1192–1198 (2013).
4. Y. N. Abdiche, R. Harriman, X. Deng, Y. A. Yeung, A. Miles, W. Morishige, L. Boustany, L. Zhu, S. M. Izquierdo, W. Harriman, Assessing kinetic and epitopic diversity across orthogonal monoclonal antibody generation platforms. *MAbs* **8**, 264–277 (2016).
5. L. M. Weiner, R. Surana, S. Wang, Monoclonal antibodies: Versatile platforms for cancer immunotherapy. *Nat. Rev. Immunol.* **10**, 317–327 (2010).
6. M. Tomita, K. Tsumoto, Recent advances in antigen-based generation of monoclonal antibodies. *Curr. Immunol. Rev.* **6**, 56–61 (2010).
7. P. Renata, A. Wadih, Hybridoma-free generation of monoclonal antibodies. *Proc. Natl. Acad. Sci. U.S.A.* **101**, 257–259 (2004).
8. M. A. Nowak, R. M. May, R. E. Phillips, S. Rowland-Jones, D. G. Lalloo, S. McAdam, P. Klenerman, B. Köppe, K. Sigmund, C. R. M. Bangham, A. J. McMichael, Antigenic oscillations and shifting immunodominance in HIV-1 infections. *Nature* **375**, 606–611 (1995).
9. L. Vijayakrishnan, V. Kumar, J. N. Agrewala, G. C. Mishra, K. V. Rao, Antigen-specific early primary humoral responses modulate immunodominance of B cell epitopes. *J. Immunol.* **153**, 1613–1625 (1994).
10. J. W. Chin, A. B. Martin, D. S. King, L. Wang, P. G. Schultz, Addition of a photocrosslinking amino acid to the genetic code of Escherichiacoli. *Proc. Natl. Acad. Sci. U.S.A.* **99**, 11020–11024 (2002).
11. Y. Zheng, M. J. Gilgenast, S. Hauc, A. Chatterjee, Capturing post-translational modification-triggered protein-protein interactions using dual noncanonical amino acid mutagenesis. *ACS Chem. Biol.* **13**, 1137–1141 (2018).
12. W. Wang, T. Li, K. Felsovalyi, C. Chen, T. Cardozo, M. Krogsgaard, Quantitative analysis of T cell receptor complex interaction sites using genetically encoded photo-cross-linkers. *ACS Chem. Biol.* **9**, 2165–2172 (2014).
13. N. Hino, Y. Okazaki, T. Kobayashi, A. Hayashi, K. Sakamoto, S. Yokoyama, Protein photo-cross-linking in mammalian cells by site-specific incorporation of a photoreactive amino acid. *Nat. Methods* **2**, 201–206 (2005).
14. M. Blech, D. Peter, P. Fischer, M. M. T. Bauer, M. Hafner, M. Zeeb, H. Nar, One target-two different binding modes: Structural insights into gevokizumab and canakinumab interactions to interleukin-1β. *J. Mol. Biol.* **425**, 94–111 (2013).
15. D. Wang, S. Zhang, L. Li, X. Liu, K. Mei, X. Wang, Structural insights into the assembly and activation of IL-1β with its receptors. *Nat. Immunol.* **11**, 905–911 (2010).
16. L. Wang, P. G. Schultz, A general approach for the generation of orthogonal tRNAs. *Chem. Biol.* **8**, 883–890 (2001).
17. J. Guo, C. E. Melancon III, H. S. Lee, D. Groff, P. G. Schultz, Evolution of amber suppressor tRNAs for efficient bacterial production of proteins containing nonnatural amino acids. *Angew. Chem. Int. Ed. Engl.* **48**, 9148–9151 (2009).
18. L. Wang, A. Brock, B. Herberich, P. G. Schultz, Expanding the genetic code of Escherichia coli. *Science* **292**, 498–500 (2001).
19. W. Liu, A. Brock, S. Chen, S. Chen, P. G. Schultz, Genetic incorporation of unnatural amino acids into proteins in mammalian cells. *Nat. Methods* **4**, 239–244 (2007).
20. J. W. Chin, Expanding and reprogramming the genetic code. *Nature* **550**, 53–60 (2017).

21. J. W. Chin, T. A. Cropp, J. C. Anderson, M. Mukherji, Z. Zhang, P. G. Schultz, An expanded eukaryotic genetic code. *Science* **301**, 964–967 (2003).
22. G. Dormán, H. Nakamura, A. Pulsipher, G. D. Prestwich, The Life of Pi Star: Exploring the exciting and forbidden worlds of the benzophenone photophore. *Chem. Rev.* **116**, 15284–15398 (2016).
23. C. M. Joiner, M. E. Breen, A. K. Mapp, Electron-deficient p-benzoyl-L-phenylalanine derivatives increase covalent chemical capture yields for protein-protein interactions. *Protein Sci.* **28**, 1163–1170 (2019).
24. T. S. Young, I. Ahmad, J. A. Yin, P. G. Schultz, An enhanced system for unnatural amino acid mutagenesis in E. coli. *J. Mol. Biol.* **395**, 361–374 (2010).
25. S. Sato, S. Mimasu, A. Sato, N. Hino, K. Sakamoto, T. Umehara, S. Yokoyama, Crystallographic study of a site-specifically cross-linked protein complex with a genetically incorporated photoreactive amino acid. *Biochemistry* **50**, 250–257 (2011).
26. J. Syed, S. Palani, S. T. Clarke, Z. Asad, A. R. Bottrill, A. M. E. Jones, K. Sampath, M. K. Balasubramanian, Expanding the zebrafish genetic code through site-specific introduction of azido-lysine, bicyclononyne-lysine, and diazirine-lysine. *Int. J. Mol. Sci.* **20**, 2577 (2019).
27. C. F. Barbas III, A. S. Kang, R. A. Lerner, S. J. Benkovic, Assembly of combinatorial antibody libraries on phage surfaces: The gene III site. *Proc. Natl. Acad. Sci. U.S.A.* **88**, 7978–7982 (1991).
28. C. F. Barbas III, R. B. Dennis, J. S. Gregg, in *Phage Display: A Laboratory Manual* (CSH Press, 2001).
29. D. Ricklin, G. Hajishengallis, K. J. Yang, Complement: A key system for immune surveillance and homeostasis. *Nat. Immunol.* **11**, 785–797 (2010).
30. W. J. Cook, N. Galakatos, W. C. Boyar, R. L. Walter, S. E. Ealick, Structure of human desArg-C5a. *Acta Crystallogr.* **66**, 190–197 (2010).
31. M. J. Toth, L. Huwyler, W. C. Boyar, A. F. Braunwalder, D. Yarwood, J. Hadala, W. O. Haston, M. A. Sills, B. Seligmann, N. Galakatos, The pharmacophore of the human C5a anaphylatoxin. *Protein Sci.* **3**, 1159–1168 (2010).
32. B. P. Morgan, C. L. Harris, Complement, a target for therapy in inflammatory and degenerative diseases. *Nat. Rev. Drug Discov.* **14**, 857–877 (2015).
33. M. S. Huber-Lang, J. V. Sarma, S. R. McGuire, K. T. Lu, V. A. Padgaonkar, E. M. Younkin, R. F. Guo, C. H. Weber, E. R. Zuiderweg, F. S. Zetoune, P. A. Ward, Structure-function relationships of human C5a and C5aR. *J. Immunol.* **170**, 6115–6124 (2003).
34. C. S. Colley, B. Popovic, S. Sridharan, J. E. Debreczeni, D. Hargeaves, M. Fung, L.-L. An, B. Edwards, J. Arnold, E. England, L. Eghobamien, U. Sivars, L. Flavell, J. Renshaw, K. Wickson, P. Warrener, J. Zha, J. Bonnell, R. Woods, T. Wilkinson, C. Dobson, T. J. Vaughan, Structure and characterization of a high affinity C5a monoclonal antibody that blocks binding to C5aR1 and C5aR2 receptors. *MAbs* **10**, 104–117 (2018).
35. A. R. M. Bradbury, J. D. Marks, Antibodies from phage antibody libraries. *J. Immunol. Methods* **290**, 29–49 (2004).
36. G. Winter, A. D. Griffiths, R. E. Hawkins, H. R. Hoogenboom, Making antibodies by phage display technology. *Annu. Rev. Immunol.* **12**, 433–455 (1994).
37. C. J. Hutchings, M. Koglin, W. C. Olson, F. H. Marshall, Opportunities for therapeutic antibodies directed at G-protein-coupled receptors. *Nat. Rev. Drug Discov.* **16**, 661 (2017).
38. C. J. Hutchings, P. Colussi, T. G. Clark, Ion channels as therapeutic antibody targets. *MAbs* **11**, 265–296 (2019).
39. D. G. Gibson, Synthesis of DNA fragments in yeast by one-step assembly of overlapping oligonucleotides. *Nucleic Acids Res.* **37**, 6984–6990 (2009).
40. R. E. Wang, Y. Wang, Y. Zhang, C. Gabrelow, Y. Zhang, V. Chi, Q. Fu, X. Luo, D. Wang, S. Joseph, K. Johnson, A. K. Chatterjee, T. M. Wright, V. T. B. Nguyen-Tran, J. Teijaro, A. N. Theofilopoulos, P. G. Schultz, F. Wang, Rational design of a Kv1.3 channel-blocking antibody as a selective immunosuppressant. *Proc. Natl. Acad. Sci. U.S.A.* **113**, 11501–11506 (2016).
41. X. Luo, G. Fu, R. E. Wang, X. Zhu, C. Zambaldo, R. Liu, T. Liu, X. Lyu, J. Du, W. Xuan, A. Yao, S. A. Reed, M. Kang, Y. Zhang, H. Guo, C. Huang, P. Y. Yang, I. A. Wilson, P. G. Schultz, F. Wang, Genetically encoding phosphotyrosine and its nonhydrolyzable analog in bacteria. *Nat. Chem. Biol.* **13**, 845–849 (2017).
42. F. Wang, D. C. Ekiert, I. Ahmad, W. Yu, Y. Zhang, O. Bazirgan, A. Torkamani, T. Raudsepp, W. Mwangi, M. F. Criscitiello, I. A. Wilson, P. G. Schultz, V. V. Smider, Reshaping antibody diversity. *Cell* **153**, 1379–1393 (2013).

Acknowledgments: We thank V. Smider, Y. Zhou, and X. Lyu for helpful discussion and Y. Chen, Z. Yang, and B. Zhou (Institute of Biophysics, CAS) for technical help with Biacore experiments. **Funding:** This work was supported, in part, by the National Key R&D Program of China (2019YFA0904200), the Strategic Priority Research Program of CAS (XDB29040202), the CAS Pioneer Hundred Talents Program, the National Key R&D Program of China (2017YFA0505400), Zhengzhou Key Laboratory of Molecular Biology, and Scientific Research Special Funds for ZZNU. **Author contributions:** L.C. and F.W. conceived the study and designed the experiments. L.C. and C.Z. performed the major parts of the experiments. R.L., L.Z., Y.S., Z.X., Z.Z., F.W., and X.L. performed experiments. L.C., C.Z., H.G., Y.Z, R.Z.M., and F.W. analyzed the data. L.C. and F.W. wrote the manuscript. **Competing interests:** The authors declare that they have no competing interests. **Data and materials availability:** All data needed to evaluate the conclusions in the paper are present in the paper and/or the Supplementary Materials. Additional data related to this paper may be requested from the authors.

Submitted 8 October 2019
Accepted 9 January 2020
Published 1 April 2020
10.1126/sciadv.aaz7825

Citation: L. Chen, C. Zhu, H. Guo, R. Li, L. Zhang, Z. Xing, Y. Song, Z. Zhang, F. Wang, X. Liu, Y. Zhang, R. Z. Ma, F. Wang, Epitope-directed antibody selection by site-specific photocrosslinking. *Sci. Adv.* **6**, eaaz7825 (2020).